Thermal Water Vapor Emission from Shocked Regions in Orion^{*}

Martin Harwit¹, David A. Neufeld², Gary J. Melnick³, and Michael J. Kaufman⁴

¹ 511 H Street S.W., Washington, DC 20024–2725

 2 Department of Physics & Astronomy, The Johns Hopkins University, 3400 North Charles Street, Baltimore, MD 21218

³ Harvard-Smithsonian Center for Astrophysics, 60 Garden Street, Cambridge, MA 02138

⁴ NASA Ames Research Center, MS 245-3, Moffett Field, CA 94035–1000

* Based on observations with ISO, an ESA project with instruments funded by ESA Member States (especially the PI countries: France, Germany, the Netherlands and the United Kingdom) with the participation of ISAS and NASA.

Subject headings: infrared: ISM: lines and bands — ISM: abundances — ISM: individual (Orion) — ISM: molecules — molecular processes

ABSTRACT

Using the Long Wavelength Spectrometer (LWS) onboard the Infrared Space Observatory (ISO), we have observed thermal water vapor emission from a roughly circular field of view approximately 75 arc seconds in diameter centered on the Orion BN-KL region. The Fabry-Perot line strengths, line widths, and spectral line shifts observed in eight transitions between 71 and 125μ m show good agreement with models of thermal emission arising from a molecular cloud subjected to a magnetohydrodynamic C-type shock. Both the breadth and the relative strengths of the observed lines argue for emission from a shock rather than from warm quiescent gas in the Orion core. Though one of the eight transitions appears anomalously strong, and may be subject to the effects of radiative pumping, the other seven indicate an H₂O/H₂ abundance ratio of order 5×10^{-4} , and a corresponding gas-phase oxygen-to-hydrogen abundance ratio of order 4×10^{-4} . Given current estimates of the interstellar, gas-phase, oxygen and carbon abundances in the solar vicinity, this value is consistent with theoretical shock models that predict the conversion into water of all the gas-phase oxygen that is not bound as CO. The overall cooling provided by rotational transitions of H₂O in this region appears to be comparable to the cooling through rotational lines of CO, but is an order of magnitude lower than cooling through H₂ emission. However, the model that best fits our observations shows cooling by H₂O and CO dominant in that portion of the post-shock region where temperatures are below ~ 800 K and neither vibrational nor rotational radiative cooling by H₂ is appreciable.

1. Introduction

The molecular hydrogen shock in the Orion BN-KL region has been intensively studied since the seminal work of Kwan and Scoville (1976) revealed emission from carbon monoxide with line widths of order 100 km s⁻¹. Following this, Beckwith *et al.* (1978) identified the rovibrational transitions of molecular hydrogen emanating from this same region. Somewhat later, Beck (1984) provided a map of the region in the (v = 0–0 S(2)) 12.3 μ m line, while studies by Watson *et al.* (1980), Stacey *et al.* (1983), and Watson *et al.* (1985) identified highly excited far-infrared rotational transitions from CO involving rotational levels ranging from J = 15 up to J = 34. Watson (1982), Viscuso *et al.* (1985), and Melnick *et al.* (1990) also studied OH transitions, with a view to understanding the dynamics and chemistry of the shocked and post-shock domains.

More recently, Sugai *et al.* (1994) have provided a detailed map of the molecular hydrogen emission. They mapped a $4' \times 4'$ region with a spatial resolving power of 5.3 arc seconds in the H₂ (v = 1–0 S(1)) transition and found substantial emission from an elongated patch roughly two minutes of arc in length and 1.5 arc minutes wide. In this region they resolved nine separate emission peaks in a structure whose outlines are roughly bipolar, straddling the central source IRc2. While many smaller peaks abound, the overall structure is generally interpreted in terms of a bipolar wind emanating from IRc2 and plowing into an ambient H₂ cloud.

Most theoretical studies of the Orion shocked region (Draine & Roberge, 1982; Chernoff, Hollenbach & McKee, 1982; Neufeld & Melnick, 1987) have concluded that a rich emission spectrum from thermally excited water vapor must be playing a significant role in cooling the gas. However, with few exceptions — such as observations of maser emission from extremely dense regions or observations of relatively low-excitation lines of the isotopomers HDO and $H_2^{18}O$ (e.g. Zmuidzinas *et al.* 1995) — the direct detection of water vapor emission has not been possible. Though thermal water vapor emission, largely confined to the far-infrared, has long been sought, telluric water vapor is an efficient absorber in the mid- and far-infrared, and blocks precisely those wavelengths at which interstellar shocks are expected to emit the bulk of their radiation. While Cernicharo *et al.* (1994) have reported detection of the 183.3 GHz radio frequency 3(1,3) - 2(2,0)transition, decisive observations had to await the launch of mid- and far-infrared spectral instrumentation into space. The Infrared Space Observatory, ISO, placed into earth orbit in November 1995, has provided a first opportunity to study these shocks systematically. Here, we provide evidence that this emission has now been reliably observed.

2. Observations

On October 6, 1997, we observed the Orion BN-KL region with ISO (cf Kessler *et al.*, 1996) from 06:02:47 to 07:58:05 UT for a total of 6918 seconds. All observations were made in the Long Wavelength Spectrometer's Fabry-Perot (LWS/FP) mode (Clegg *et al*, 1996). The instrument's roughly circular field of view was centered on the epoch 2000 coordinates $5h 35m 14.2s, -5^{\circ} 22' 23.3$ ".

We obtained data on eight H₂O lines. These detections required the use of four different detectors, each having its own roughly elliptical beam size — 70 × 68 arc seconds at 125 and 121 μ m, 77 × 71 at 99.5, 95.6 and 90 μ m, 82 × 76 at 83 and 82 μ m, and 83 × 79 at 72 μ m. The fields of view, therefore, differed by ±19%.

In the wavelength range from 72 to 125 μ m the LWS/FP's spectral resolving power gradually increases from ~ 7,000 to a peak of ~ 9,800 at 95 μ m, before slowly dropping to ~ 9,500 at 125 μ m. We repeatedly stepped the Fabry-Perot over a wavelength range that spanned 5 resolution elements on either side of each line. This made for a total of 11 resolution elements, each of which was sampled at 8 equally spaced positions within the element, in what is designated as the "rapid scanning" mode of operation, each measurement lasting only 0.5 sec. Strong signals were observed in all eight lines (see Figure 1).

3. Results

The main observational results are listed in Table 1. The first two columns, respectively, identify the transitions observed and indicate whether the line is emitted by ortho- or

para- H_2O . The third column gives the wavelength. The fourth column lists the line center displacement in terms of velocity with respect to the local standard of rest. Like all the other observational parameters listed in Table 1, this was determined from a Gaussian line fit. Since the spectral resolving power of the Fabry-Perot spectrometer ranges from 9,000 to 7,000, the lines necessarily are broader than 33 to 43 km s⁻¹. The relatively small spread of central line velocities observed, $\pm 8 \text{ km s}^{-1}$, probably is due to noise, and suggest that all of the lines are emitted from one and the same region. Inspection of Figure 1, where the observed line profiles are displayed, visually confirms the quality of the data and shows the small statistical errors that arise in comparing the many scans taken over each of the lines. Column 5 of Table 1 gives the line widths. These widths are of the order of 60 km s^{-1} full width at half maximum, significantly exceeding the minimum line width of $33 \text{ to } 43 \text{ km s}^{-1}$ determined by the spectral resolving power. They are consistent with an intrinsic line-of-sight velocity distribution that is Gaussian with full-width-half-maximum \sim 35 km s⁻¹, convolved with the Fabry-Perot's Lorentzian profile at the above-stated resolving power. This estimate of the intrinsic line width is supported by additional observations toward Orion Peak 1 to be reported elsewhere. These made use of ISO's Short Wavelength Spectrometer, whose resolving power of ~ 31,000 displayed a 42 km s⁻¹ full-width-half-maximum velocity distribution in the $4_{32} - 3_{03}$ H₂O emission line at 40.69 $\mu m.$

Column 6 of Table 1 shows the total flux measured in each line. Columns 7 and 8 involve theoretical modeling and are discussed below. Column 9, the last column, provides the detected continuum level. It is substantial, and underscores the importance of correct continuum subtraction. At 100 μ m a flux of ~ 1.5×10^5 Jy corresponds to ~ 5×10^{-17} W cm⁻² per resolution element, comparable to the total line flux.

The calibration of the LWS/FP is a complex procedure that continues to be refined. It consists, in first place, of a calibration of the LWS detector response in the instrument's grating mode. This is periodically monitored through the use of five infrared illuminators incorporated into the instrument, and by observing selected astronomical calibration sources. The response in the Fabry-Perot mode, for which the grating serves as an order sorter, is then deduced primarily from a preflight calibration of the Fabry-Perot etalon's added transmission losses.

As seen in the line plots of Fig. 1, the continuum appears to be steep for some of the lines. A variety of factors contribute to these slopes. They include changes in the transmission function of the blocking filters and grating, a changing detector response function, and interference effects within the instrument that lead to sizeable fringe amplitudes. To the extent that our continuum levels agree with continuum observations obtained by others, they nevertheless provide us with a means of ascertaining the reliability of the line fluxes we list.

Werner *et al.* (1976) mapped the same region of Orion we observed, with a field of view one arc minute in diameter, and described its spectrum as a blackbody at 70 K with a $20 \,\mu m/\lambda$ emissivity. We find rough agreement in the spectral distribution of our continuum values with the spectral shape they describe. Moreover, the peak flux Werner et al. observed at 100 μ m with a 40 μ m bandwidth was 9 \times 10⁴ Jy. The continuum flux levels listed in Table 1 were all obtained with larger fields of view, but if we roughly prorate our observed flux to the smaller field of view of Werner *et al.*, taking into account that their maps show a rapid decrease in flux away from the peak, we derive respective fluxes of $\sim 0.64, \sim 1.25$ and $\sim 1.57 \times 10^5$ Jy at 121.7, 99.49 and 82.03 μ m. Since these three values provide a rough sampling of their wavelength range, we can average them to obtain a mean value ~ 1.15×10^5 Jy or 25% higher. Werner *et al.* estimated the uncertainties in their absolute flux levels at $\pm 20\%$. Summing the two uncertainties of 25 and 20\% in quadrature, we obtain an uncertainty in the continuum fluxes listed in Table 1, of $\sim \pm 35\%$. On the basis of this comparison we estimate our line fluxes to be similarly uncertain by $\sim \pm 35\%$. As the Long Wavelength Spectrometer characteristics become better established in the next few months, this error budget may be revised.

4. The Model

The luminosity of water vapor emission from the Orion shock was predicted by Kaufman & Neufeld (1996) [hereafter KN] and in Kaufman's PhD thesis (1995). Their model solved for the equilibrium populations of the lowest 179 rotational levels of ortho-H₂O and for the lowest 170 rotational levels of para-H₂O. The model included cooling due to rovibrational transitions of H₂O, H₂ and CO, and due to dissociation of H₂. Cooling through gas-grain collisions was also included.

Water vapor in shocks is formed through reactions of atomic oxygen with molecular hydrogen to form OH radicals, which subsequently react with hydrogen molecules to form water vapor (Elitzur & de Jong, 1973; Elitzur & Watson, 1978). Once the shock-generated temperatures exceed ~ 400 K, the KN model predicts that all the oxygen not already incorporated in CO will be converted into H₂O. This is shown by computations that predict the relative abundances of the primary oxygen-bearing species, H₂O, OH, O, and O₂ throughout the shock. Expected spectral line emission from each of these species is computed using an escape probability formalism. The calculations included emission from the lowest 60 rotational states of ¹²CO as well as ¹³CO, and the lowest 21 rotational states of H₂. For both molecular hydrogen and water vapor, the ortho/para ratio was assumed to be 3:1. Vibrational transitions from states up to v = 2 for CO and H₂ were included, as were ν_2 band transitions of H₂O.

In order for a shock not to dissociate interstellar molecules, the cloud through which it passes must be able to cool itself appreciably more quickly than it is heated by the shock. This will generally happen only if a magnetic field is present and pre-compresses the medium in what Draine (1980) has termed a continuous or "C-type" shock. This more gradual compression becomes possible because the Alfvén speed exceeds the speed of sound in the cloud. A magnetic precursor penetrates the cloud before the arrival of a J-type shock front in the wake of which temperatures and densities could sharply jump to dissociate the molecules.

KN considered a C-shock and predicted the H₂O emission from Orion assuming the gas-phase oxygen and carbon abundances of Pollack *et al.* (1994), which were premised on Solar System elemental abundances, and a model of the shocked region in Orion based on data primarily obtained in CO and H₂ observations. These indicated a best fit for a shock velocity $v_s = 37 \text{ km s}^{-1}$ and a preshock H₂ density of 10^5 cm^{-3} . These values were constrained by the observed line-strength ratios of two pairs of spectral lines — the CO (J=34–33) and (J=21–20) lines and the H₂ (v = 1–0 S(1)) and (v = 2–1 S(1)) lines.

The shock velocity and hydrogen density do not depend on the assumed oxygen abundance, but the expected water vapor density does. Based on the work of Pollack *et al.* (1994), KN assumed the gas phase abundances of oxygen and carbon nuclei to be, respectively, 5.45×10^{-4} and 1.2×10^{-4} relative to hydrogen nuclei. This led to the prediction that the water vapor abundance would be as high as $n(H_2O)/n(H_2) = 8.5 \times 10^{-4}$, and that the H₂, H₂O, and CO lines, respectively should radiate away 75, 21 and 4% of the shock energy. More recent data by Cardelli *et al.* (1996) [hereafter CMJS], however, indicate that the gas phase in diffuse interstellar clouds within 600 pc of the Sun exhibits a remarkably constant abundance of carbon and oxygen, with $n(O)/n(H) = 3.16 \times 10^{-4}$ and $n(C)/n(H) = 1.4 \times 10^{-4}$. In a preliminary calculation applied to Orion, we find that this substantially lower oxygen abundance predicts a correspondingly reduced water vapor concentration, $n(H_2O)/n(H_2) \sim 3.5 \times 10^{-4}$, and a drop in water vapor cooling that is close to proportional to the drop in abundance. The H₂ : H₂O : CO cooling ratios thus become 88 : 8 : 4.

To determine the expected H_2O flux from Orion, we still need to know the value of a projection parameter which KN call Φ . It is the ratio of the actual surface area of the shock(s) to the projected area of the beam at the distance of the source. For a complex region the field of view may contain n shocks and the function Φ is summed over all of them. For a beam-filling, planar shock $\Phi = 1$; for a beam-filling, spherical shock its value is $\Phi = 4$.

Observationally, the value of Φ is derived as the ratio of the radiant energy observed, to the mechanical inflow energy expected for a beam-filling planar shock seen face-on. For the Orion shock, we infer the value of Φ from an estimate of the total surface brightness in our 75 arc second field of view, summed over all H_2 emission lines. To this end, we use Beck's (1984) $H_2(v = 0 - 0 S(2))$ intensity averaged over the observed field of view as a tracer for the total H_2 emission — much of which is not directly observable because it is extinguished by ambient dust. Beck's data averaged over our field of view give a $12.3 \,\mu\text{m}$ intensity of $\sim 1.6 \times 10^{-3} \,\mathrm{erg} \,\mathrm{cm}^{-2} \,\mathrm{s}^{-1} \,\mathrm{sr}^{-1}$, when corrected by a factor of ~ 2 for 0.75 mag of extinction. The KN model indicates that the $12.3 \,\mu \text{m}$ flux needs to be multiplied by a factor of ~ 530, under the assumed density and shock velocity conditions, to yield a total intensity summed over all H_2 spectral lines. Though this multiplier is large, we have confidence that it is quite accurate and that it reliably implies a total H₂ intensity of $\sim 0.85 \,\mathrm{erg}\,\mathrm{cm}^{-2}\,\mathrm{s}^{-1}\,\mathrm{sr}^{-1}$. Assuming that this is 88% of the total cooling, we would expect a total radiated flux from all species of $\sim 0.97 \,\mathrm{erg}\,\mathrm{cm}^{-2}\,\mathrm{s}^{-1}\,\mathrm{sr}^{-1}$. This has to be compared to the kinetic energy inflow, which is $\text{nmv}^3/8\pi \sim 0.92 \,\text{erg}\,\text{cm}^{-2}\,\text{s}^{-1}\,\text{sr}^{-1}$. The ratio of these two quantities yields $\Phi \sim 1.05.$

We are now in a position to compare the observed H₂O fluxes to the predicted. Table 11 of KN predicts the flux in a field of view 44 arc seconds in diameter for a shock with $\Phi \sim 3$. This field of view subtends a solid angle 0.34 times that of our ~ 75 arc second field. The H₂O abundances predicted using the gas-phase abundances from CMJS are only 0.41 times as high as the values KN had assumed. These three effects partially cancel, but we have to divide the values listed in Table 11of KN by 2.5 in order to apply their results to our observations with a 75 arc second beam.

Column 7 of Table 1 lists the ratios of the observed fluxes to the adjusted KN predictions based on the CMJS abundances. Given the wide range of energies E at which the upper levels for the transitions lie, $300 \leq E \leq 800$ K, it is unlikely that the observed-to-predicted line ratios would accidentally happen to fall into the narrow range in column 7 for all but one of the eight lines observed. Our abundance estimate assumes that the water line emission originates entirely in the shocked gas component, and not in a lower temperature region. This is confirmed both by the line-strength ratios and by the observed line widths. Rigorous calculations, which we do not present here, confirm that the predicted H₂O fluxes scale almost linearly with H₂O abundance, though the average value of the actual-to-predicted line flux in column 7 drops by about 6% and the inferred abundances correspondingly rise by ~ 6%. For the substantial uncertainties in our flux

calibrations, in our estimate of Φ , and in the abundance estimates, this agreement is reasonable. The deviant 121.7 μ m line flux may reflect the neglect of radiative pumping by dust continuum radiation in the KN model. Preliminary calculations show that pumping by the ambient radiation field of Werner *et al.* raises the flux in this one line and leaves the other transitions essentially unaffected. Disregarding the anomalous 121 μ m flux, we see that the observed values are roughly 30% higher than the predicted values.

5. Discussion

Molecular shocks are important not only for their intrinsic interest, but also because current views assume that star formation may well be triggered by shock compression followed by rapid cooling. The cooling needs to be rapid in order to prevent a quasi-elastic bounce which would permit shock-compressed regions to rebound to their original dimensions. If a shocked region is able to radiate away a substantial fraction of its energy during the traversal time of the shock, it will remain compressed. Even if it is not sufficiently dense at this stage to enter protostellar collapse, it will be poised to contract further if subjected to subsequent shocks.

We can estimate the integrated water vapor line flux from Orion summed over all transitions and compare it to the power radiated away by H₂ and CO. To estimate the total water vapor emission we can sum the flux both from lines that we have observed and lines whose strengths we infer by applying the KN model. This leads us to deduce a total water vapor emission of ~ 0.11 erg cm⁻² s⁻¹ sr⁻¹ normalized to a 75 arc second diameter solid angle. The beam-averaged CO flux from the region is ~ 0.13 erg cm⁻² s⁻¹ sr⁻¹ obtained from the observational data cited in Stacey *et al.*(1983), normalized to an assumed beam size of 60 arc seconds — slightly smaller than the beam size used for our H₂O observations. This value could, however, drop by ~ 35% if the shocked region subtended a substantially smaller solid angle than our 75 arc second beam. The H₂O and CO cooling of the shocked region are therefore comparable; but both are an order of magnitude lower than the total H₂ emission.

6. Conclusions

We have observed water vapor emission from the shocked region in Orion, and find that the detected flux is consistent with a model proposed by Kaufman & Neufeld (1996), which inferred a shock velocity of ~ 37 km s⁻¹ and a pre-shock H₂ density of ~ 10^5 cm⁻³. However the model can only be correct if we assume a water vapor abundance $n(H_2O)/n(H_2) \sim 5 \times 10^{-4}$ and a corresponding interstellar gas-phase oxygen abundance $n(O)/n(H) \sim 4 \times 10^{-4}$, in agreement with values cited by CMJS, in place of a substantially higher Solar System abundance inferred from Pollack *et al* (1994). Water vapor cooling in the shock is comparable to CO cooling, but amounts to only $\sim 10\%$ of the total cooling provided by molecular hydrogen emission. Nevertheless, the KN model shows that H₂O and CO should dominate in that portion of the post-shock region where temperatures are ≤ 800 K and neither vibrational nor rotational radiative cooling of H₂ is appreciable.

We wish to thank Steven Lord at IPAC and members of the LWS consortium in the UK for their advice on LWS data-reduction techniques. We also thank members of the helpdesk at Vilspa for their support. Michael Werner, the paper's referee made a number of clearly helpful comments. M. H. is pleased to acknowledge NASA grant NAG5-3347 to Cornell University; D. A. N has been supported by NASA grant NAG5-3316. G. J. M. would like to cite support through NASA LTSA grant NAG5-3542 and contract NAS5-30702, and M. J. K. is pleased to acknowledge support from NASA RTOP 344-04-10-02 and RTOP 864-03-08-90.

References

- Beck, S. C. 1984, ApJ, 281, 205
- Beckwith, S., Persson, S. E., Neugebauer, G., & Becklin, E. E. 1978, ApJ, 223, 464
- Cardelli, J. A., Meyer, D. M., Jura, M., & Savage, B. D. 1996, ApJ, 467, 334
- Cernicharo, J. Gonzáles-Alfonso, E., Alcolea, J. Bachiller, R., & John D. 1994, ApJ, 432, L59
- Chernoff, D. F., Hollenbach, D. J., & McKee, C. F. 1982, ApJ, 259, L97
- Clegg, P. E. et al. 1996, A&A 315, L36
- Draine, B. T., 190, ApJ 241, 1021
- Draine, B. T., & Roberge, W. G. 1982, ApJ, 259, L91
- Elitzur, M., & de Jong, T. 1973 A&A, 67, 323
- Elitzur, M., & Watson, W. D. 1978, A&A, 70, 443
- Kaufman, M. J. 1995, PhD Thesis, Johns Hopkins University
- Kaufman, M. J., & Neufeld, D. A. 1996, ApJ, 456, 611
- Kessler, M. F., Steinz, J. A., Anderegg, M. E., Clavel, J., Drechsel, G., Estaria, P., Faelker, J., Riedinger, J. R., Robson, A., Taylor, B. G., & Xim'enez de Ferrán, S. 1996, A&A, 315, L27
- Kwan, J., & Scoville, N. Z. 1977, ApJ, 210, L39
- Melnick, G. J., Stacey, G. J., Genzel, R., Lugten, J. B., & Poglitch, A. 1990, ApJ, 348, 161
- Neufeld, D. A., & Kaufman, M. J. 1993, ApJ, 418, 263
- Neufeld, D. A., & Melnick, G. J. 1987, ApJ, 332, 266
- Pollack, J. B., Hollenbach, D., Beckwith, S., Simonelli, D. P., Roush, T., & Fong, W. 1994, ApJ, 421, 615
- Stacey, G. J., Kurtz, N. T., Smyers, S. D., & Harwit, M. 1983, MNRAS, 202, 25p
- Sugai, H., Usuda, T., Kataza, H., Tanaka, M., Inoue, M. Y., Kawabata, H., Takami, H., Aoki, T., & Hiromoto, N. 1994, ApJ, 420, 746
- Viscuso, P. J., Stacey, G. J., Fuller, C. E., Kurtz, N. T., & Harwit, M. 1985, ApJ, 296, 142
- Watson, D. M., Storey, J. W. V., Townes, C. H., Haller., E. E., & Hansen, W. L. 1980, ApJ, 239, L129

Watson, D. M. 1982, PhD Thesis, University of California, Berkeley.

Watson, D. M., Genzel, R., Townes, C. H., & Storey, J. W. V. 1985, ApJ, 298, 316

- Werner, M. W., Gatley, I., Harper, D. A., Becklin, E. E., Loewenstein, R. F., Telesco, C. M., & Thronson, H. A., 1976, ApJ, 204, 420
- Zmuidzinas, J., Blake, G.A., Carlstrom, J., Keene, J., Miller, D., Schilke, P., and Ugras, N.G. 1995, in *Proceedings of the Airborne Astronomy Symposium on the Galactic Ecosystem: From Gas to Stars to Dust*, eds. M. R. Haas, J. A. Davidson & E. F. Erickson (San Francisco: ASP), p. 33

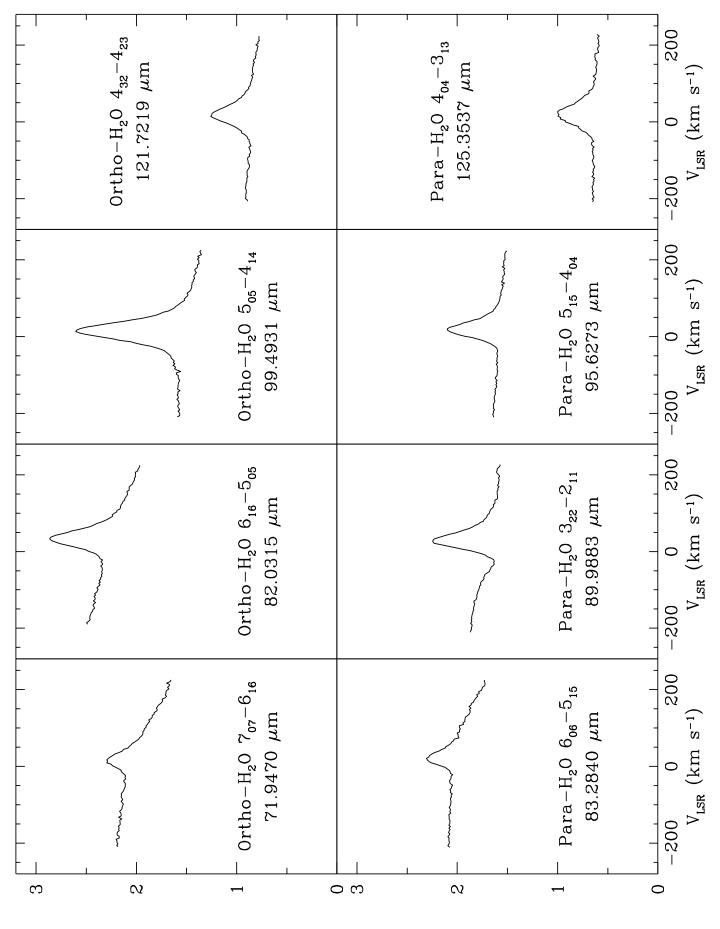
| LWS lines observed toward Orion BN/KL | | | | | | | | |
|---------------------------------------|-------|-----------|---------------------------|---------------------------|-----------------------|------------|------------------------------------|---------------------|
| Line | | λ | $V_{\rm LSR}$ | ΔV | Line Flux | Line Flux/ | Inferred | Continuum |
| | | | | | | KN-CMJS | Abundance | Flux |
| | | (μm) | $({\rm km} {\rm s}^{-1})$ | $({\rm km} {\rm s}^{-1})$ | $(W \text{ cm}^{-2})$ | Prediction | $n(\mathrm{H_2O})/n(\mathrm{H_2})$ | (Jy) |
| $4_{04} - 3_{13}$ | Para | 125.3537 | 21 | 70 | 2.2×10^{-17} | 1.0 | 3.5×10^{-4} | 6.2×10^{4} |
| $4_{32} - 4_{23}$ | Ortho | 121.7219 | 27 | 65 | 2.2×10^{-17} | 5.2 | 1.8×10^{-3} a | 8.5×10^4 |
| $5_{05} - 4_{14}$ | Ortho | 99.4931 | 17 | 70 | $7.4 	imes 10^{-17}$ | 1.4 | $4.9 	imes 10^{-4}$ | $1.5 	imes 10^5$ |
| $5_{15} - 4_{04}$ | Para | 95.6273 | 23 | 50 | $2.8 	imes 10^{-17}$ | 1.5 | $5.3 	imes 10^{-4}$ | $1.6 	imes 10^5$ |
| $3_{22} - 2_{11}$ | Para | 89.9883 | 33 | 54 | 3.7×10^{-17} | 1.85 | 6.5×10^{-4} | $1.6 	imes 10^5$ |
| $6_{06} - 5_{15}$ | Para | 83.2840 | 27 | 45 | 1.6×10^{-17} | 1.3 | 4.6×10^{-4} | $2.0 	imes 10^5$ |
| $6_{16} - 5_{05}$ | Ortho | 82.0315 | 22 | 61 | 4.8×10^{-17} | 1.2 | $4.2 	imes 10^{-4}$ | $2.2 	imes 10^5$ |
| $7_{07} - 6_{16}$ | Ortho | 71.9470 | 23 | 64 | $2.6 	imes 10^{-17}$ | 1.1 | $3.8 	imes 10^{-4}$ | $2.0 	imes 10^5$ |

Table 1 LWS lines observed toward Orion BN/KI

 a This abundance estimate should be regarded as an upper limit, because the 121.7 μ m line flux is significantly enhanced by radiative pumping, a process neglected in the KN model.

Figure Caption

Fig. 1 – Line profiles of the observed transitions listed in Table 1. Error bars showing standard deviations from a mean obtained in successive spectral scans are too small to be discerned on this scale. Corrections, however, were made by eliminating grossly deviant data points resulting from cosmic ray impacts on detectors. Given the large number of scans obtained, these subtractions did not significantly alter the final results.



Flux / 105 Jy

Flux / 105 Jy